Broadband quasiphasematching for large-scale entanglement in the quantum optical frequency comb

Pei Wang,* Wenjiang Fan, and Olivier Pfister
Department of Physics, University of Virginia, Charlottesville, Virginia 22903, USA

We observed a remarkably broad sum frequency generation quasiphasematching bandwidth in periodically poled $KTiOPO_4$, in the 1058-1070 nm wavelength and 15-40 °C temperature ranges. The quasiphasematching efficiency was constant over 3.178(2) THz, only limited by laser tuning range. This is consistent with our theoretical prediction of a 4.74 THz quasiphasematching full width at 99% maximum near the 9μm poling period in PPKTP. This broad phasematching bandwidth is key to defining very large (10,000-qumode) quantum computing registers by creating continuous-variable cluster states in the quantum optical frequency comb.

arXiv:1403.6631v1 [physics.optics] 26 Mar 2014

I. INTRODUCTION

Quantum computing [1] can be implemented, among other options, with quantum optics [2–5] and in particular using, in lieu of qubits, the continuous variables defined by individual quantum oscillator modes of the electromagnetic field [6, 7]. These modes are characterized by their quadrature amplitude operators which are the analogues of the position and momentum of a harmonic oscillator $\hat{q} = (\hat{a} + \hat{a}^\dagger)/\sqrt{2}$, $\hat{p} = (\hat{a} - \hat{a}^\dagger)/(i\sqrt{2})$, where $\hat{a}$ is the photon annihilation operator of a particular mode. Operators $\hat{q}$ and $\hat{p}$ have a continuous spectrum. An interesting particular implementation uses the quantum optical frequency comb (QOFC) of an optical parametric oscillator (OPO) [8, 9], whose important feature is its "top-down" scalability potential. This has been demonstrated experimentally by entangling a world-record 60 modes of the QOFC of a single OPO [10, 11]. (Note that 10,000 modes were also entangled sequentially in a different work, but were only accessible 2 modes at a time [12].) In the QOFC experiments, the OPO modes are spaced by a free spectral range of 0.95 GHz and the OPO's nonlinear crystal provides entanglement by way of two-mode squeezing. The number of entangled modes is therefore given by the ratio of the phasematching bandwidth of the OPO crystal and of the free spectral range. In this Letter, we studied, theoretically and experimentally, quasiphasematched parametric downconversion (PDC) in periodically poled $KTiOPO_4$ (PPKTP) pumped at 532 nm. The experimental study used sum-frequency generation. We show that the quasiphasematching is very broad and flat, with a 4.74 THz full width, at 99% of the maximum efficiency. This would yield 10,000 entangled OPO modes of both orthogonal polarizations.

II. THEORY

We model quasiphasematched (QPM) [13–15] zzz sum frequency generation (SFG) in PPKTP, which is identical to the PDC used in OPO-based quantum computing registers, and lends itself more easily to experimental characterization. We follow the standard plane-wave treatment in the slowly varying amplitude approximation, all classical fields being of the form $E_j = A_j e^{-i(k_j x - \omega_j t)}$, $j \in [1, 5]$. Two monochromatic, linearly polarized input fields $E_{1,2}$ at frequencies $\omega_{1,2}$ travel in the crystal along its x axis and give rise to SFG field E_3 at $\omega_3 = \omega_1 + \omega_2$, as well as SHG fields $E_{4,5}$ at $2\omega_1$ and $2\omega_2$. The coupled wave equations are

$$\frac{da_1}{dx} = -ig_1 a_1^* a_4 e^{-i\Delta k_1 x} - ig_3 a_2^* a_3 e^{-i\Delta k_3 x} \quad (1)$$

$$\frac{da_2}{dx} = -ig_2 a_2^* a_5 e^{-i\Delta k_2 x} - ig_3 a_1^* a_3 e^{-i\Delta k_3 x} \quad (2)$$

$$\frac{da_3}{dx} = -ig_3 a_1 a_2 e^{i\Delta k_3 x} \quad (3)$$

$$\frac{da_4}{dx} = -i\frac{g_1}{2} a_1^2 e^{i\Delta k_3 x} \quad (4)$$

$$\frac{da_5}{dx} = -i\frac{g_2}{2} a_2^2 e^{i\Delta k_3 x} \quad (5)$$

where $a_j = A_j/\sqrt{2\eta_j \hbar\omega_j}$, $\eta_j = \eta_0/n_j$ is the impedance of the medium, $g_{1,2}^2 = 4\hbar\omega_{1,2}^3 \eta_{1,2}^2 \eta_{4,5} d_{33}^2$, $g_3^2 = 2\hbar\omega_1\omega_2\omega_3\eta_1\eta_2\eta_3 d_{33}^2$, and d_{33} is the second-order nonlinear coefficient. The SHG and SFG phase mismatches are, respectively,

$$\Delta k_{1,2} = n(2\omega_{1,2}, T)\frac{2\omega_{1,2}}{c} - 2n(\omega_{1,2}, T)\frac{\omega_{1,2}}{c} - \frac{2\pi}{\Lambda}, \quad (6)$$

$$\Delta k_3 = n(\omega_3, T)\frac{\omega_3}{c} - n(\omega_1, T)\frac{\omega_1}{c} - n(\omega_2, T)\frac{\omega_2}{c} - \frac{2\pi}{\Lambda}, \quad (7)$$

where Λ is the poling period. In the limit of undepleted pumps $a_{1,2}$, Eqs. (1-5) can be solved simply to yield the total intensity

$$I = g_3^2 L^2 |a_1 a_2|^2 \operatorname{sinc}^2\Big(\frac{\Delta k_3 L}{2}\Big) + \frac{g_1^2}{4} L^2 |a_1|^4 \operatorname{sinc}^2\Big(\frac{\Delta k_1 L}{2}\Big) + \frac{g_2^2}{4} L^2 |a_2|^4 \operatorname{sinc}^2\Big(\frac{\Delta k_2 L}{2}\Big). \quad (8)$$

We first examine the SFG phasemismatch of Eqs. (8) & (7) at room temperature as a function of the poling

* pw4cq@virginia.edu

period Λ and of SFG input — or OPO "signal" — frequencies ω_1 and $\omega_2 = \omega_3 - \omega_1$, ω_3 being fixed to the pump frequency (563 THz, 532 nm) of the OPO. This can be done by using temperature-dependent Sellmeier equations [16, 17]. The result, plotted in Fig. 1, displays

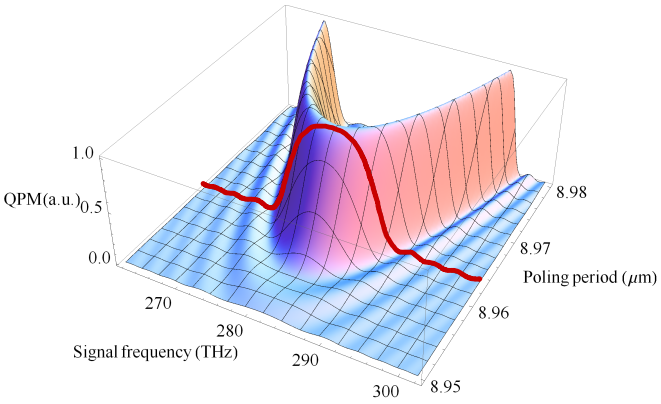

FIG. 1. Quasiphasematching function, versus signal frequency ω_1 and poling period, for a 1 cm-long PPKTP crystal. The red line outlines the considered QPM FWHM bandwidth, which reaches 4.74 THz at 99% of the maximum and decreases significantly in the separated branches.

a remarkably broad phasematching frequency bandwidth around frequency degeneracy ($\omega_1 = \omega_2 = \omega_3/2$). Therefore, we can expect a 532 nm pumped, zzz PPKTP OPO to achieve mode entanglement over a 4.74 THz full width at 99% maximum, which would yield 10,000 entangled cavity modes for an OPO of 0.95 GHz free spectral range.

III. EXPERIMENT AND RESULTS

In order to test this prediction, we used experimental SFG with 2 Newport-New Focus TLB-6721 "Velocity" tunable, continuous-wave, linearly polarized diode lasers, the sum of whose frequencies was kept constant over a 1058-1070 nm wavelength range. The experimental setup is shown in Fig. 2. The x-cut, $1 \times 2 \times 10$ mm^3 PPKTP

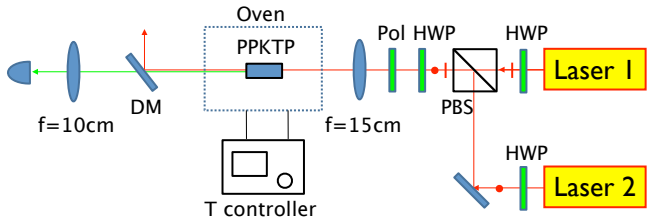

FIG. 2. Experimental setup. HWP: half wave plate; PBS: polarizing beam splitter; Pol: polarizer; DM: dichroic mirror (HR for IR and AR for green).

crystal was poled at a period of 9.0 μm (at room temperature) and provided by Raicol Crystals. The crystal faces were antireflection coated by Advanced Thin Films for both y and z polarizations at 1064 nm and for the z polarization at 532 nm. The PPKTP crystal was placed in a temperature-stabilized oven, controlled by a Peltier module driven by a Wavelength Electronics, Model LFI-3751 temperature controller.

The power of the lasers are set to be 23.0(2) mW and 19.6(2) mW, respectively, to compensate the efficiency difference caused by their different beam profiles. The power of the z-polarized beam entering the crystal are 7.7(2) mW and 7.0(2) mW respectively. Both lasers were scanned in the wavelength range of 1058-1070 nm, keeping the average wavelength of the two lasers fixed at 1064.090(5) nm, so that the generated SFG green beam always had $\lambda = 532.05$ nm. The IR frequencies displayed by each laser were initially measured with a Coherent WaveMaster wavelength meter for calibration.

Figure 3(a) shows the measured power of generated green beam (both SFG and SHG) versus the fundamental wavelength and crystal temperature. For each temperature, about 30 data points of different wavelength are measured. The maximum SFG and SHG power were 19.2(1) nW and 8.94(1) nW respectively, yielding maximum efficiencies for SFG and SHG of $3.60(2)\times10^{-4}$ W^{-1} and $1.67(1) \times 10^{-4}$ W^{-1}, respectively. We attributed these relatively modest values to the unoptimized overlap of the highly elliptical transverse intensity profiles of the diode lasers. However, we believe it is reasonable to assume that this imperfect overlap was stationary throughout the measurements.

Figure 3(b) shows the theoretical prediction for the total green intensity. As can be clearly seen, the qualitative behavior of SHG (frequency-sharp ridges) and SFG (broadband feature) match the experimental results very well. The measured frequency width of the constant SFG QPM was 3.178(2) THz, at least, since our measurement was limited by the tuning range of the diode lasers (we could not make use of the full 1030-1070 nm tuning range of the lasers as it was not centered on the SHG fundamental wavelength of 1064 nm).

IV. CONCLUSION

We have demonstrated broadband quasiphasematching of sum-frequency generation, i.e., also of parametric downconversion, in 9μm-poled PPKTP for 532/1064 nm up/down-converted wavelengths. The 3.178(2) THz measured QPM bandwidth, at constant SFG efficiency, was limited by the tunability of our diode lasers and hence this result is only a lower bound for the actual QPM bandwidth. As it stands, this measurement indicates that 10,000 cavity modes (beyond the 60 actually measured) should be entangled as recently demonstrated in a single OPO [11]. Analogous calculations for longer wavelengths, such as 775/1550 nm, indicate that the QPM bandwidth at 99% of the maximum should be broader there by a factor of 3. Note that even broader quasiphasematching has been achieved for SFG using noncollinear

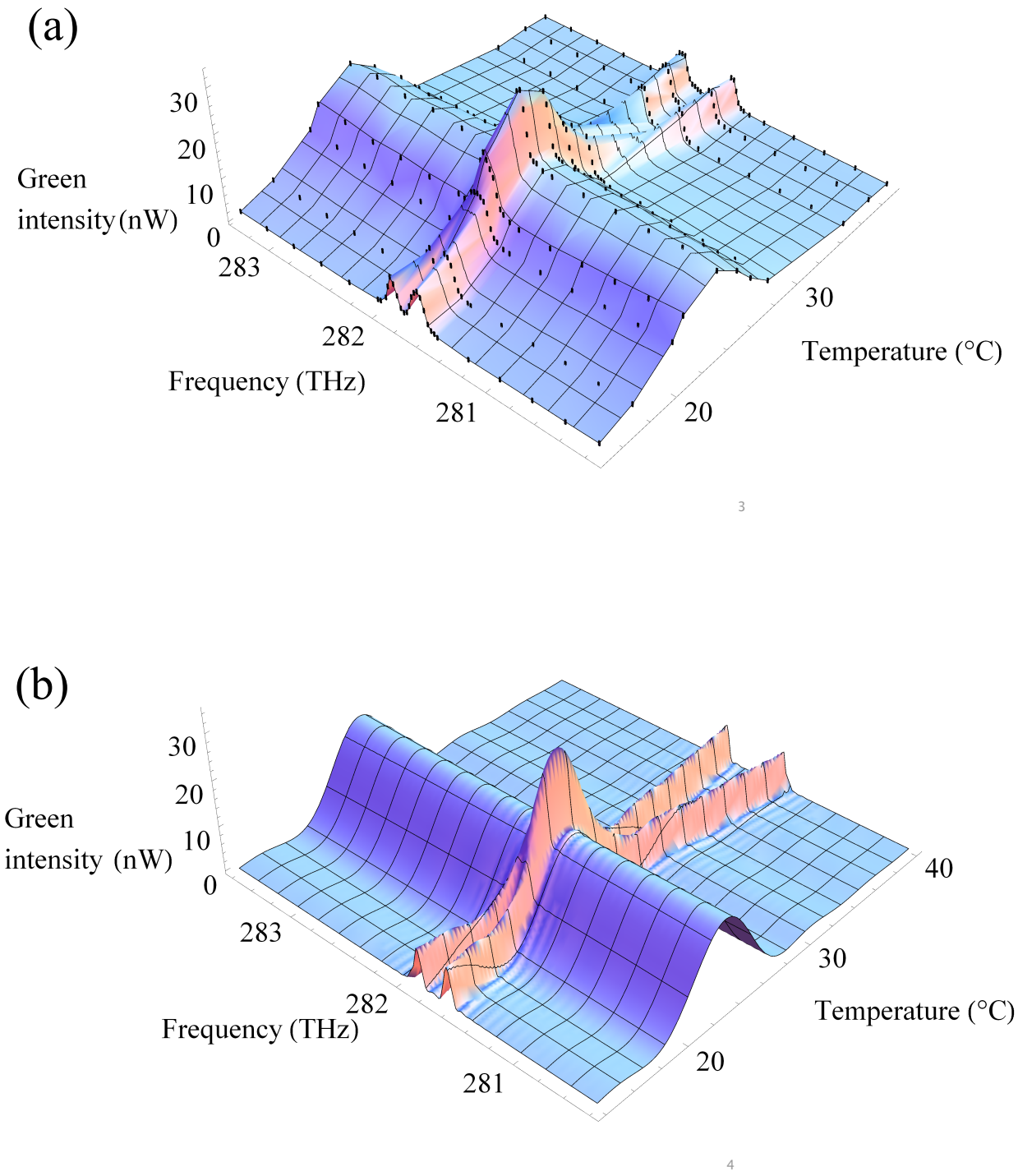

FIG. 3. (a) Experimental phasematching curve. The laser wavelength is scanned from 1058 to 1070 nm, the temperature of the crystal is scanned from 15°C to 40°C (11 different temperatures). For each temperature, about 30 data points of different wavelength are measured. The 3D plot is interpolated from the data points. (b) Theoretical phasematching curve, plotted by using the respective power values 18.28 nW for $g_3^2L^2|a_1a_2|^2$, and 8.23 nW for $g_1^2L^2|a_1|^4 = g_2^2L^2|a_2|^4$ in Eq. (8). The measured SFG bandwidth is 3.178(2) THz, at quasi-constant efficiency, around 23°C. The crossing ridges are due to the more narrowly quasiphasematched SHG interactions.

beams [18]. Here, we have simply limited ourselves to the characterization of the experimental situation of Refs. 10 and 11, which requires collinear modes modematched to the same OPO cavity.

We thank Moran Chen for discussions. This work was supported by the U.S. National Science Foundation under grant No. PHY-1206029.

[1] T. D. Ladd, F. Jelezko, R. Laflamme, Y. Nakamura, C. Monroe, and J. L. O'Brien, "Quantum computers," Nature (London) **464**, 45 (2010).

[2] S. Lloyd and S. L. Braunstein, "Quantum computation over continuous variables," Phys. Rev. Lett. **82**, 1784 (1999).

[3] S. D. Bartlett, B. C. Sanders, S. L. Braunstein, and K. Nemoto, "Efficient classical simulation of continuous variable quantum information processes," Phys. Rev. Lett. **88**, 097904 (2002).

[4] N. C. Menicucci, P. van Loock, M. Gu, C. Weedbrook, T. C. Ralph, and M. A. Nielsen, "Universal quantum computation with continuous-variable cluster states," Phys. Rev. Lett. **97**, 110501 (2006).

[5] N. C. Menicucci, "Fault-tolerant measurement-based quantum computing with continuous-variable cluster states," Phys. Rev. Lett., in press. arXiv:1310.7596 [quant-ph] (2013).

[6] S. L. Braunstein and P. van Loock, "Quantum information with continuous variables," Rev. Mod. Phys. **77**, 513 (2005).

[7] C. Weedbrook, S. Pirandola, R. García-Patrón, N. J. Cerf, T. C. Ralph, J. H. Shapiro, and S. Lloyd, "Gaussian quantum information," Rev. Mod. Phys. **84**, 621–669 (2012).

[8] O. Pfister, S. Feng, G. Jennings, R. Pooser, and D. Xie, "Multipartite continuous-variable entanglement from concurrent nonlinearities," Phys. Rev. A **70**, 020302 (2004).

[9] N. C. Menicucci, S. T. Flammia, and O. Pfister, "One-way quantum computing in the optical frequency comb," Phys. Rev. Lett. **101**, 130501 (2008).

[10] M. Pysher, Y. Miwa, R. Shahrokhshahi, R. Bloomer, and O. Pfister, "Parallel generation of quadripartite cluster entanglement in the optical frequency comb," Phys. Rev. Lett. **107**, 030505 (2011).

[11] M. Chen, N. C. Menicucci, and O. Pfister, "Experimental realization of multipartite entanglement of 60 modes of a quantum optical frequency comb," Phys. Rev. Lett., in press. arXiv:1311.2957 [quant-ph] (2014).

[12] S. Yokoyama, R. Ukai, S. C. Armstrong, C. Sornphiphatphong, T. Kaji, S. Suzuki, J. ichi Yoshikawa, H. Yonezawa, N. C. Menicucci, and A. Furusawa, "Ultra-large-scale continuous-variable cluster states multiplexed in the time domain," Nat. Photon. **7**, 982 (2013).

[13] J. A. Armstrong, N. Bloembergen, J. Ducuing, and P. S. Pershan, "Interactions between light waves in a nonlinear dielectric," Phys. Rev. **127**, 1918 (1962).

[14] M. M. Fejer, G. A. Magel, D. H. Jundt, and R. L. Byer, "Quasi-phase-matched second harmonic generation: tuning and tolerances," IEEE J. Quantum Electron. **28**, 2631 (1992).

[15] L. E. Myers, R. C. Eckardt, M. M. Fejer, R. L. Byer, W. R. Bosenberg, and J. W. Pierce, "Quasi-phase-matched optical parametric oscillators in bulk periodically poled $LiNbO_3$," J. Opt. Soc. Am. B **12**, 2102 (1995).

[16] K. Fradkin, A. Arie, A. Skliar, and G. Rosenman, "Tunable midinfrared source by difference frequency generation in bulk periodically poled $KTiOPO_4$," Appl. Phys. Lett. **74**, 914–916 (1999).

[17] S. Emanueli and A. Arie, "Temperature-dependent dispersion equations for $KTiOPO_4$ and $KTiOAsO_4$," Appl. Opt. **42**, 6661 (2003).

[18] A. Pe'er, Y. Bromberg, B. Dayan, Y. Silberberg, and A. A. Friesem, "Broadband sum-frequency generation as an efficient two-photon detector for optical tomography," Opt. Express **15**, 8760–8769 (2007).